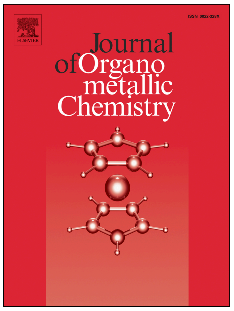

Covalent functionalization and solubilization of multi-walled carbon nanotubes by using zinc and copper complexes of meso-tetra(4-aminophenyl) porphyrin

G. Prabhavathi, R. Yamuna, Alifia C. Jafer

PII: S0022-328X(18)30130-X
DOI: 10.1016/j.jorganchem.2018.02.031
Reference: JOM 20330

To appear in: *Journal of Organometallic Chemistry*

Received Date: 16 September 2017
Revised Date: 6 February 2018
Accepted Date: 21 February 2018

Please cite this article as: G. Prabhavathi, R. Yamuna, A.C. Jafer, Covalent functionalization and solubilization of multi-walled carbon nanotubes by using zinc and copper complexes of meso-tetra(4-aminophenyl) porphyrin, *Journal of Organometallic Chemistry* (2018), doi: 10.1016/j.jorganchem.2018.02.031.

Covalent Functionalization and Solubilization of Multi-walled Carbon Nanotubes by Using Zinc and Copper Complexes of Meso-tetra(4-aminophenyl) porphyrin

G. Prabhavathi[a], R. Yamuna*[b] and Alifia C. Jafer[b]

[a] Research and Development Centre, Bharathiar University, Coimbatore – 641 046, India. [b]Center of Excellence in Advanced Materials and Green Technologies (CoE-AMGT), Dept. of Sciences, Amrita School of Engineering, Coimbatore, Amrita Vishwa Vidyapeetham, India. ryamuna1@gmail.com.

1. Introduction

Carbon nanotubes (CNTs) stand out as distinctive materials owing to their variety of physical and chemical properties such as high surface area, high electrical and thermal conductivity, structural integrity, significant mechanical strength and chemical inertness [1-3]. CNTs are used as electrode materials in electrochemical devices in order to promote electron transfer reactions [4,5]. Literature studies show that cobalt corrole adsorbed on the surface of multiwalled carbon nanotubes (MWCNTs) demonstrated an exceptional electro-catalytic property towards the reduction of oxygen [6]. Furthermore, cobalt-porphyrin complex that attached to multiwalled carbon nanotubes (CNTs) have shown higher catalytic performance for oxygen-reduction reaction (ORR) in acidic medium, indicating the advantages of supramolecular complex formed by electro-catalytic metalloporphyrin covalently linked to CNTs [7]. Recent studies on heterogeneous nano catalysts containing iron (III) porphyrin covalently attached onto the surface of MWCNTs showed to be an efficient catalyst in the epoxidation of alkene under mild conditions [8]. Zhao *et. al.* constructed a sensor for the detection of nitrite in water sample by immobilizing hemoglobin on MWCNTs modified glass carbon electrode [9]. Recent studies have also shown that MWCNT-based nanohybrid systems in which MWCNTs are covalently functionalized with dye molecules as electron donor-acceptor ensembles (D-A) have attracted intense scientific interest due to their enhanced photo-electronic properties [10,11]. MWCNTs are preferred to other carbon nanomaterials as components of electron (D-A) ensembles due to the presence of large number of concentric graphitic tubes. Nevertheless, the use of MWCNTs in building various photovoltaic and non-linear optical (NLO) materials have been impeded due to their poor solubility in most of the organic and aqueous solvents and also difficulties associated with processing. Therefore, significant effort has been devoted towards the covalent functionalization of MWCNTs with chromophoric molecules in order to simultaneously promote the solubility and also to improve the photo-electronic properties of the nano-hybrid [12,13].

Porphyrins have fascinated significant attention for applications in solar cells and molecular electronics in owing to their interesting biological, optical, electronic and structural properties [14-16]. These molecules possess unique optoelectronic properties due to the small reorganization energies and this, together with their large π-conjugated systems [17]. Fine tuning of these properties can be achieved through varying the substituents at the macrocyclic periphery or central metal ion [18]. Literature study also shows that covalently functionalized metalloporphyrin (Zn or Cu) with carbon nanomaterials exhibited enhanced NLO and optical limiting properties [19-21].

In this paper, covalent functionalization of 5,10,15,20-meso-tetra(4-aminophenyl)porphyrinato Zn (II) complex (Zn-TAP, Chart 1) and 5,10,15,20-meso-tetra(4-aminophenyl)porphyrinato Cu (II) complex (Cu-TAP, Chart 1) with MWCNTs (nano hybrid **(I)** and (**II**), respectively) through an amide linkage has been reported. The chemical structure of synthesized nano hybrids I and II have been testified by Raman, Fourier transform infrared (FT-IR) and X-ray photoelectron (XPS) spectroscopy. Thermal stability of these nano hybrids were studied by thermogravimetric analysis (TGA). Morphology of the nano hybrids were analysed by Transmission electron microscopy (TEM). Linear optical studies of these nano hybrids are reported.

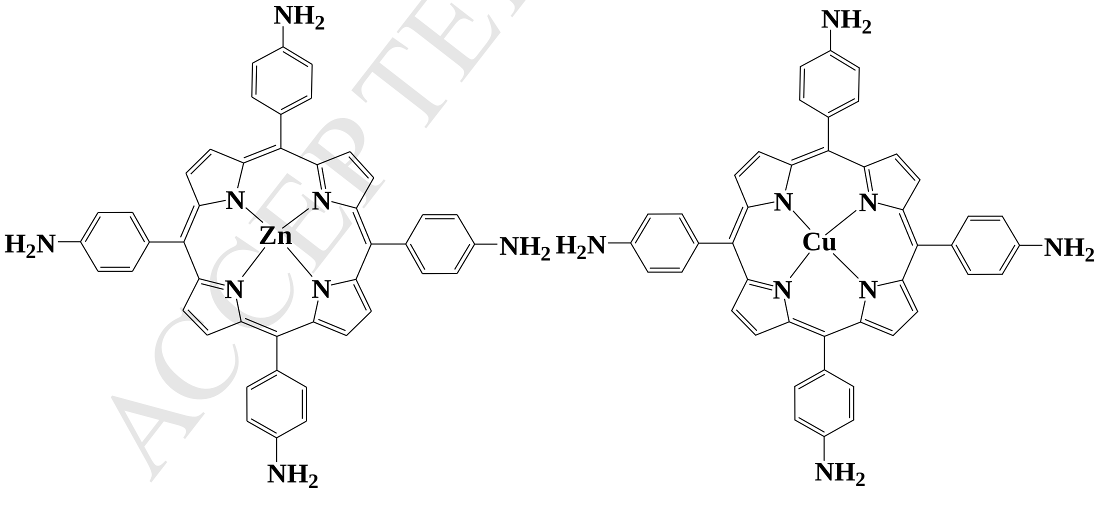

(a) **(b)**

Chart 1. Chemical structure of a) Zn-TAP and b) Cu-TAP

2. Materials and Methods

2.1. Materials

Pyrrole, Zinc (II) acetate dihydrate and copper (II) acetate monohydrate were purchased from Merck. Other reagents such as chloroform ($CHCl_3$), dry tetrahydrofuran (THF, Finar) and N,N-dimethylformamide (DMF) were purified by using standard procedures. MWCNTs were purchased from Yunnan Great (Group) Co., Ltd. (China). Carboxyl functionalized MWCNTs (MWCNT–COOH) and TAP were synthesized by using the literature procedure [22].

2.2. Characterization and Instrumentation

Fourier transform infrared spectra (FT-IR) were measured on a Thermo Nicolet, iS10 FT-IR spectrophotometer using KBr pellet method. Thermogravimetric analysis (TGA) was carried out using SDT Q600 simultaneous DSC-TGA with a heating rate of 5 ^{o}C/min under N_2 purge (100 ml/min). Absorption studies were carried out with a SHIMADZU, UV-1800 UV spectrophotometer. Nuclear magnetic resonance (NMR) spectra were measured on a 500 MHz Bruker NMR spectroscopy using tetramethylsilane (TMS) as the internal standard. The chemicals shifts were expressed in parts per million (ppm). Raman spectra were obtained from the micro Raman spectroscopy (The CRAIC Technologies™). Photo emission spectra were obtained by using a SHIMADZU RF-6000 spectrofluorophotometer. JEOL JEM 2100 high resolution transmission electron microscopy (HR-TEM) instrument was used to record the TEM images of nano-hybrid. X-ray photoelectron spectroscopy (XPS) analysis was performed in KRATOS Axis Ultra (Kratos Analytical, Manchester, United Kingdom). Electron spin resonance (EPR) spectrum was recorded in Varian E112 spectrometer.

2.3. Synthesis of 5,10,15,20-meso-tetra(4-aminophenyl) porphyrinato Zn (II) complex:

Zinc (II) acetate dihydrate (0.227 g, 1.034 mmol) and 5, 10, 15, 20-mesotetra(4-aminophenyl) porphyrin (0.100 g, 0.148 mmol) were refluxed in DMF solvent (15 mL) for 3 h at 80 ^{o}C. Thin layer chromatography (TLC) was used to check the completion of reaction. Rota-evaporator was used to remove the excess DMF solvent. Further the residue was purified by washing five times with water (15 mL) through sintered crucible in order to remove excess zinc acetate and other impurities from the product. Finally, trituration of the crude product with ethyl acetate (5 mL) and followed by drying the product under vacuum afforded the title compound as purple solid. Yield: 0.072 g, 80 %. ^{1}H nuclear magnetic resonance spectroscopy (^{1}H NMR) in d^{6}-

dimethylsulfoxide (d^6-DMSO): 5.42 (s, 8H), 6.95 (d, 8H), 7.79 (d, 8H), 8.81 (m, 8H) (see supporting information Figure.S1).

2.4. Synthesis of 5,10,15,20-meso-tetra(4-aminophenyl) porphyrinato Cu (II) complex:

5, 10, 15, 20-mesotetra-(4-aminophenyl) porphyrin (0.050 g, 0.074 mmol) was refluxed with copper (II) acetate monohydrate (0.207 g, 1.036 mmol) in dimethylsulfoxide (15 mL) at 100 ^{0}C for 4 h. After completion of the reaction as indicated by TLC, the DMSO solvent was removed by using rota-evaporator. Further the residue was purified by washing five times with water (15 mL) through sintered crucible in order to remove excess copper (II) acetate and other impurities from the product. Finally, trituration of the crude product with ethyl acetate (5 mL) and followed by drying the product under vacuum afforded title compound. Yield: 75%. The formation of the complex has been confirmed by the electron spin resonance (EPR) spectrum recorded in DMF solvent at room temperature. The g_{II} value < 2.3 indicates a co-ordinate covalent character of the Cu-N bonds in the copper-porphyrinic complexes (see supporting information Figure S2).

2.5. Synthesis of MWCNT-CONH-ZnTAP nano hybrid

MWCNT–COOH (100 mg) was refluxed at 70 ^{o}C for 24 h with $SOCl_2$ (75 mL) under argon atmosphere in the presence of DMF (1.8 mL) to form acyl chloride functionalized MWCNT (MWCNT–COCl). Excess $SOCl_2$ was removed by vacuum distillation and the remaining residue was washed with dry THF. MWCNT–COCl (100 mg) and Zn-TAP (100 mg) were dissolved in DMF (30 mL). Further this mixture was refluxed at 130 ^{o}C for 72 h in presence of 1 mL triethylamine (Et_3N) under argon atmosphere. The resultant solution was cooled to room temperature. Excess DMF were removed by using rotary evaporator. 100 ml of ether was added into the reaction mixture in order to precipitate the product. The residue was separated through ultracentrifugation. Finally, the precipitate was purified by washing with THF (3 mL) and further washed five times with $CHCl_3$ which is followed by filtration in order to remove excess Zn-TAP and other impurities from the residue. TLC was used to check the filtrate to confirm the absence of Zn-TAP in the final washing. The resultant product was washed with water in order to remove $Et_3N.HCl$ from the nano hybrid and it was dried under vacuum.

2.6. Synthesis of MWCNT-CONH-CuTAP nano hybrid

MWCNT-CuTAP nano hybrid (**2a**) was synthesized by following the above procedure by using Cu-TAP instead of Zn-TAP.

3. Result and discussion

3.1. Synthesis of materials

Zn-TAP and Cu-TAP were synthesized by refluxing their corresponding acetate salts with TAP in DMF and DMSO, respectively. Zn-TAP and Cu-TAP were covalently linked to MWCNT through an amide bond by refluxing the porphyrin complex with MWCNT–COCl at 130 ^{o}C for 72 h in DMF solvent under argon in presence of triethylamine (Et_3N) as shown in the scheme 1.

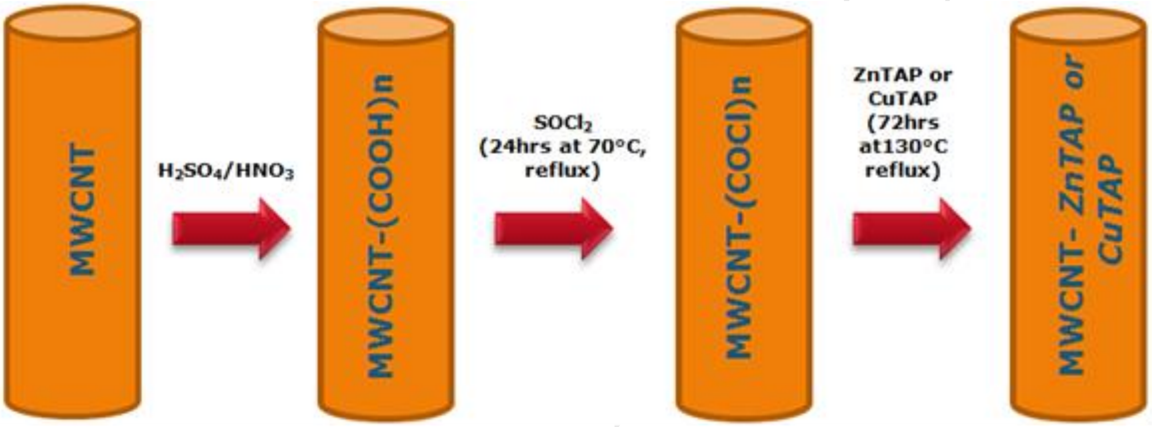

Scheme1. Reaction scheme for the covalent functionalization of MWCNTs with Zn-TAP and Cu-TAP

The chemical structure of nano-hybrids I and II were testified by FT-IR spectra as shown in Figure 1. In FT-IR spectra, MWCNT–COOH reveal characteristic peak at 3414 cm^{-1} which is attributed to the O–H vibration frequency. The peak at 1709 cm^{-1} in MWCNT-COOH is attributed to the carbonyl (C=O) stretching frequency of carboxyl moieties (COOH). This peak is shifted to 1688 cm^{-1} and 1692 cm^{-1} in the nano-hybrids I and II, respectively due to the formation of amide bond (–CO-NH-). Whereas this (C=O) peak in nano-hybrid I and II are slightly shifted to higher frequency compared to that of MWCNT-TAP (1638 cm^{-1}) [22]. The N-H stretching and bending vibration frequencies of the porphyrinic core for TAP appeared at ~ 3330 cm^{-1} and 963 cm^{-1}, respectively [22]. Whereas these two peaks are nearly disappeared in Zn-TAP and Cu-TAP which is owing to the replacement of hydrogen atom in the N-H bond by metal ions [23]. Whereas a strong peak observed near 1000 cm^{-1} which corresponds to the skeletal ring vibration of metal substituted porphyrin [24]. The peak at ~ 3380 cm^{-1} in Zn-TAP and Cu-TAP is owing to the N-H stretching frequency of amino (–NH$_2$) group. Furthermore nano hybrids I and II also show single broad band at 3415 and 3433 cm^{-1}, respectively due to the N-H stretching mode of (–CO–NH, -NH$_2$). Two more new striking bands appeared in the nano-hybrids I and II at 1256, 1586 and 1237, 1599 cm^{-1}, respectively which is attributed to the stretching vibration of C-N of amide bond and porphyrin C=C, respectively [25,26]. These noticeable modifications in the FT-IR spectra reveal the formation of covalently connected nano hybrids I and II (separate FT-IR spectra are given in the supporting information Figures S3 and S4 for clarity). Furthermore FT-IR spectra of Cu-TAP and nano hybrid II show higher frequency shift in their peaks compared to Zn-TAP and its nano hybrid, indicating different electronic interaction of metal ions.

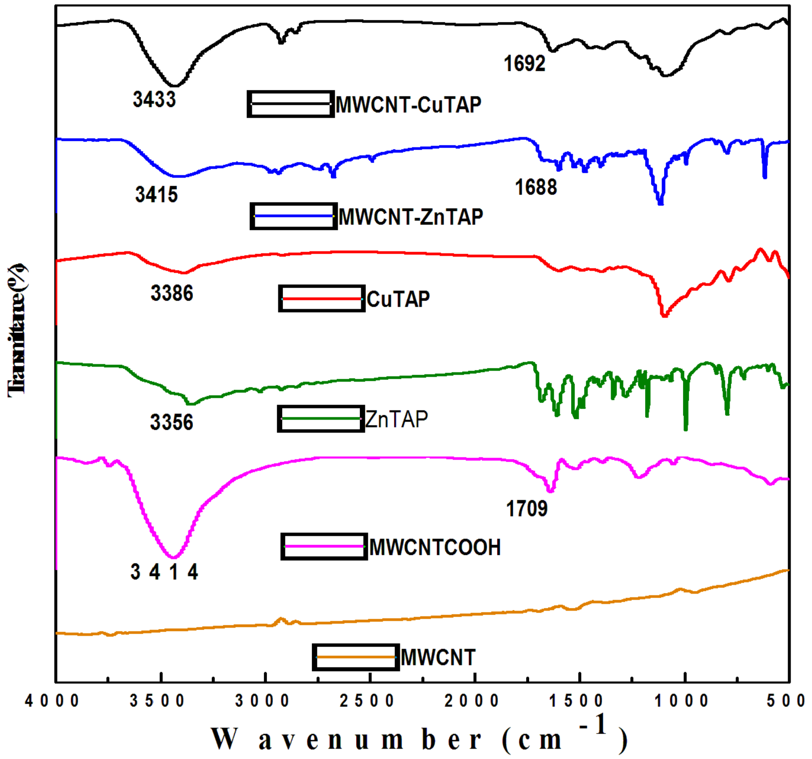

Figure.1. FT-IR spectra of MWCNT, MWCNTCOOH, Zn-TAP, Cu-TAP, MWCNT-ZnTAP (I) and MWCNT-CuTAP (II)

Figure.2. depicts the Raman spectra of MWCNT, MWCNT-COOH, nano hybrids I and II. All these materials show two Raman bands in the first order region. In general, the band appeared at ~1300 cm^{-1} is often called as the D-band and another band centered at ~1500 cm^{-1} is known as the tangential G-band. The D-band is attributed to the structural defects or disorder present in the graphitic sp^2-hybridized carbon systems. However G-band is related to the planar stretching vibrational mode of graphitic carbon atoms [18]. The second order Ǵ- or 2D-band which appear around 2600 cm^{-1} is corresponds to the overtone of the D-band. The ratio of D band intensity relative to that of the G band (I_D/I_G) is utilized as a method to assess the quality of nanotubes. MWCNT, MWCNT-COOH, nano hybrids I and II exhibit I_D/I_G ratio of 0.93, 1.06, 0.96 and 1.01, respectively. After covalent functionalization with Zn-TAP or Cu-TAP, the intensity of D band of nano hybrids I and II was reduced compared with MWCNT-COOH. Furthermore, there is a slight increase in the I_D/I_G ratio of MWCNT-ZnTAP or MWCNT-CuTAP as compared to that of MWCNT and MWCNT-TAP [22]. Similarly, D and G bands position of MWCNT-COOH, MWCNT-ZnTAP, and MWCNT-CuTAP exhibit higher frequency shift (stiffening) compared with MWCNT. This higher frequency shift in nano hybrids I and II is possibly due to the metal which acts as Lewis acid owing to its co-ordination with TAP molecule that acts as Lewis base. These observations are clear evidence for the chemical functionalization of MWCNTs, subsequently Raman spectroscopy is very sensitive to the electronic structure.

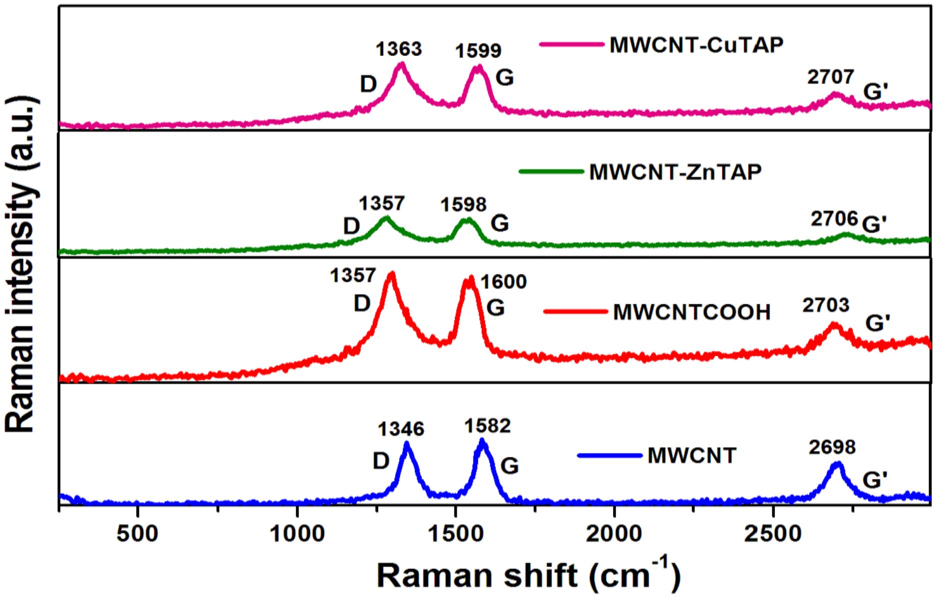

Figure.2. Raman spectra of MWCNT, MWCNT-COOH, MWCNT-ZnTAP and MWCNT-CuTAP

TGA has been widely employed to study the upper temperature limit of a material and also for the determination of covalent functionalization of MWCNTs. TGA results of MWCNT, MWCNT-COOH, ZnTAP, CuTAP, nano hybrids I and II are shown in the Figure.3. TGA plot reveals that MWCNT, Cu-TAP and Zn-TAP are thermally more stable and shows less than 20 % weight loss in the temperature range 50-800 ^{o}C. TGA plot of MWCNT-COOH reveals that 27 % weight loss in the temperature range of 50–500 ^{o}C which is attributed to the elimination of physisorbed water, decarboxylation, removal of –OH and other metal impurities on the surface of MWCNT–COOH. Nano hybrids I and II show approximately 40 and 23 % weight loss in the temperature range of 180-800 ^{o}C, respectively. This weight loss relates to the loss of Zn-TAP or Cu-TAP from the nano hybrids which were covalently linked to the MWCNTs. Nano hybrid II shows more thermal stability compared to nano hybrid I and also compared to the reported similar nano hybrids [18,22].

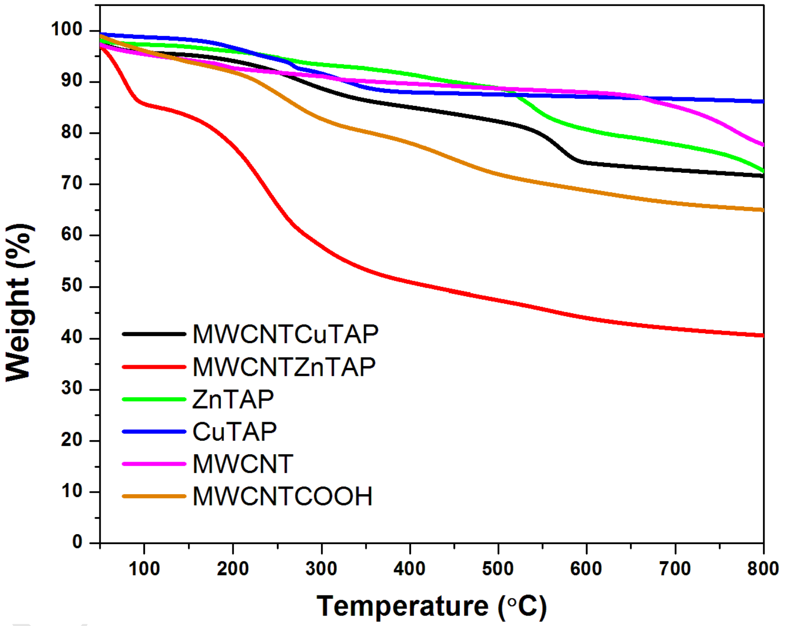

Figure.3. TGA curves of MWCNTCOOH, MWCNT, Cu-TAP, Zn-TAP, MWCNT-ZnTAP (I) and MWCNT-CuTAP (II)

Morphology study of two nano hybrids I and II have been carried out by using HR-TEM analysis. Images showing the morphology of MWCNT, MWCNT-COOH, nano hybrids I and II are presented in the Figures 4 and 5. As shown in Figure 4a, the surface of the pure MWCNTs is relatively smooth and tubular structure can be clearly distinguished. However, the observed dark spot in the magnified image of MWCNT (Figure 4b) indicates the presence of amorphous carbon [27]. Tem images of MWCNT-COOH (Figure 4c and 4d) indicate the decrease in the quantity of amorphous carbon. Whereas the Figure 4c shows the presence of defect sites along the MWCNT side walls due to oxidation. Nevertheless, after functionalization with Zn-TAP or Cu-TAP as shown in the Figure 5, the MWCNTs surfaces became rougher and also the observed dark spots on the surface of carbon nanotubes clearly reveal the metalloporphyrin functionalization (see supporting information Figure S5). Tubular morphology was retained even after functionalization.

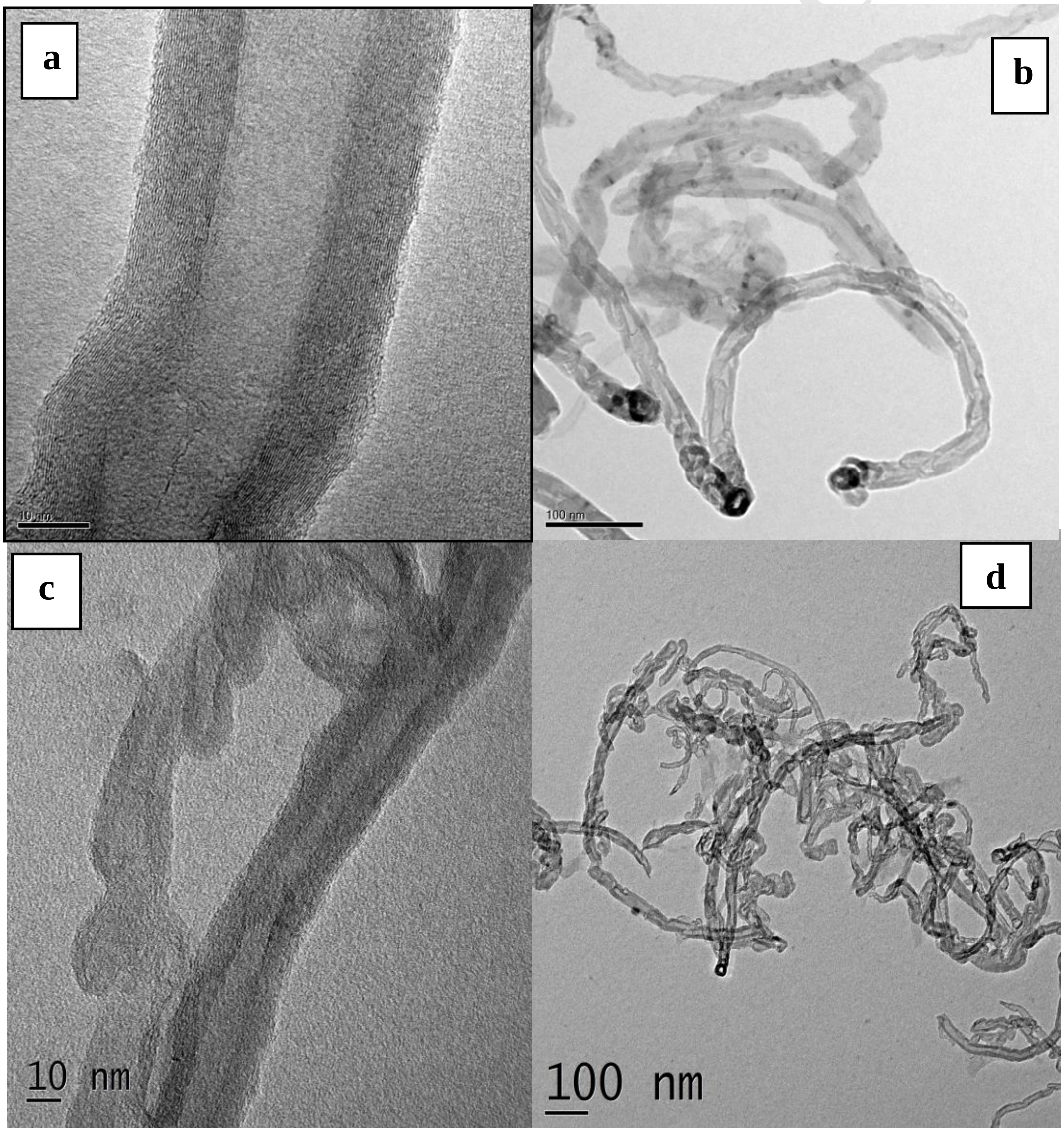

Figure.4. TEM images of (a & b) MWCNT (c & d) MWCNT-COOH

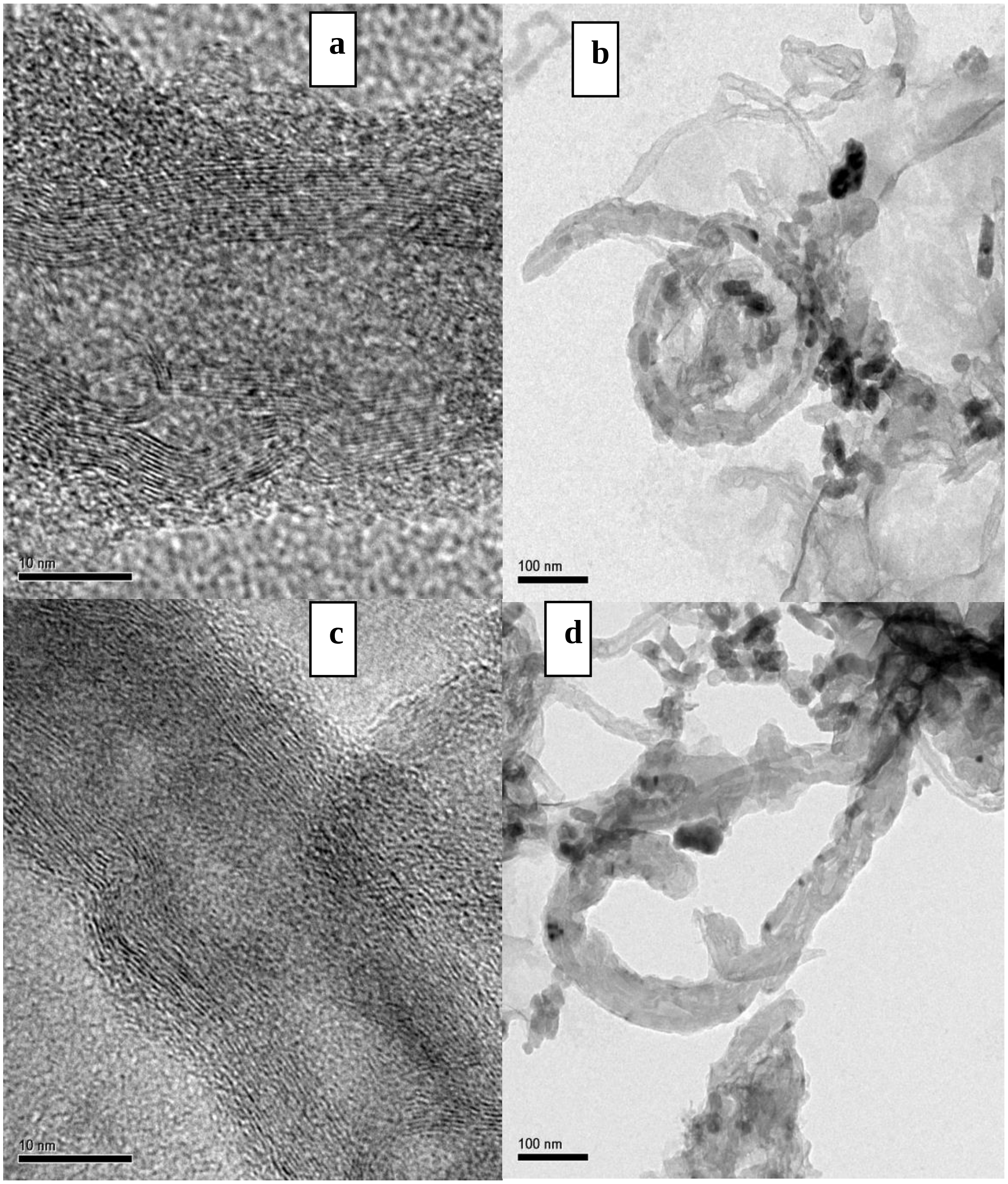

Figure.5. TEM images of (a & b) MWCNT-ZnTAP (I) and (c & d) MWCNT-CuTAP (II)

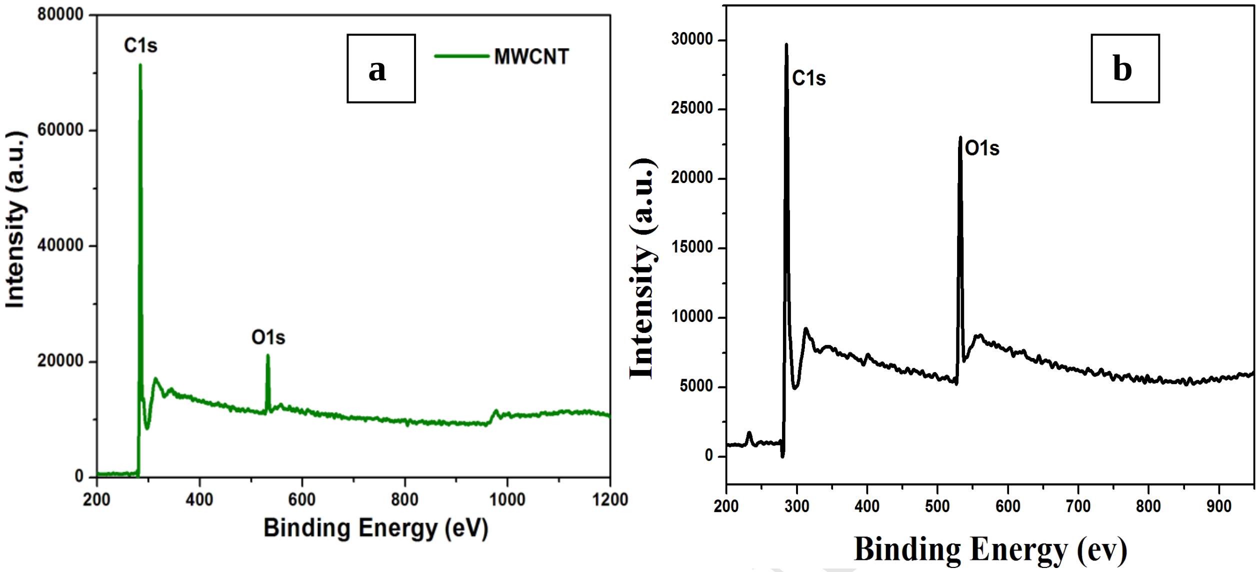

Figure.6. XPS spectra of a) MWCNT & b) MWCNT-COOH

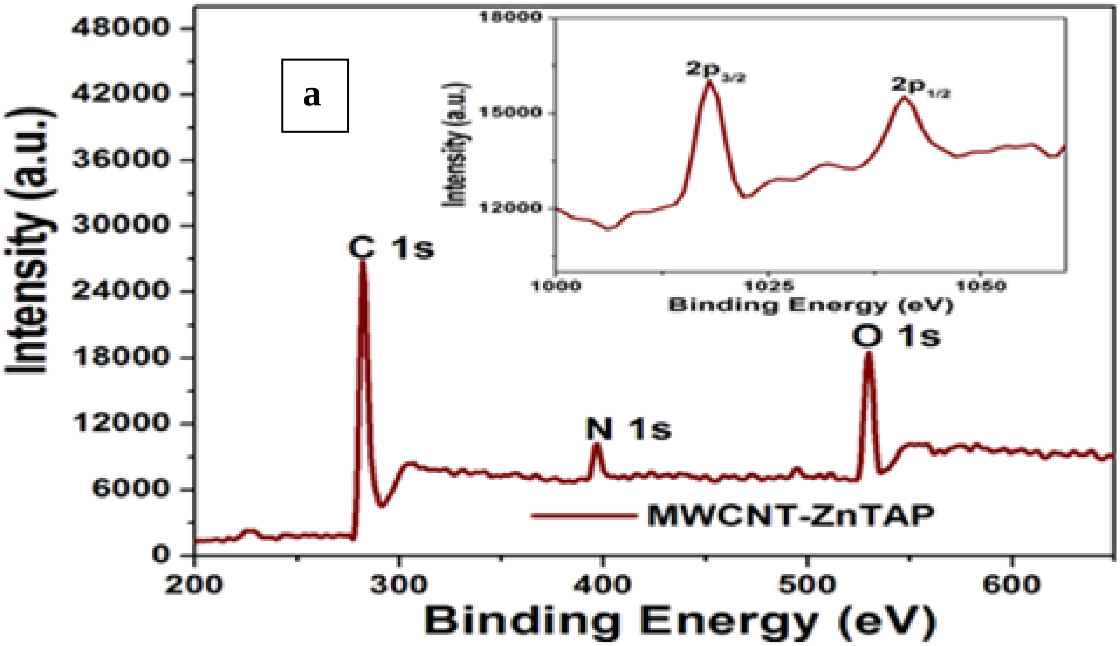

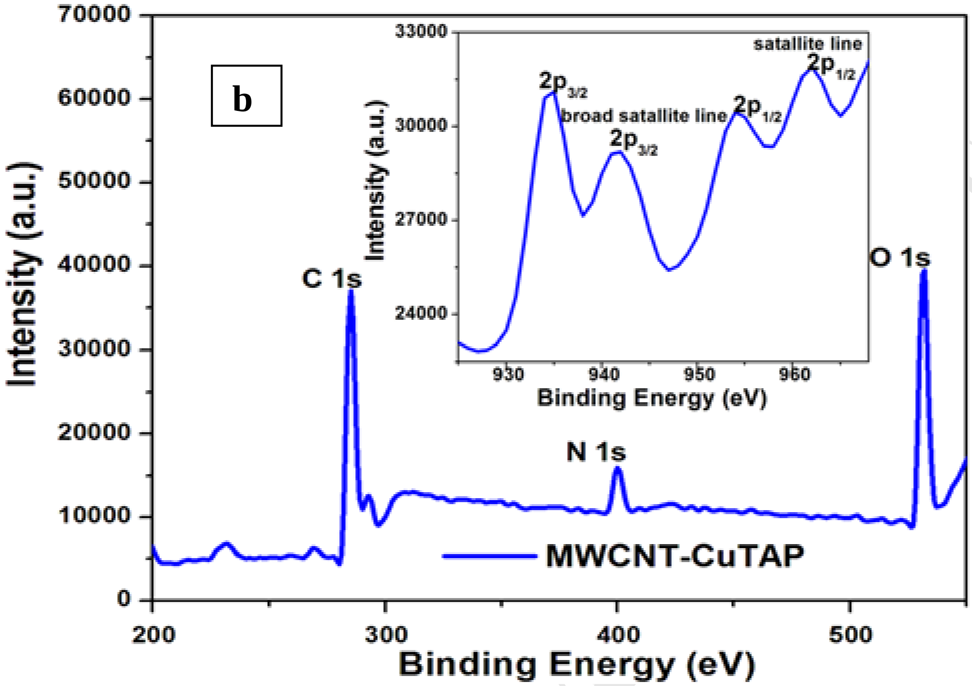

Figure.7. XPS spectra of a) MWCNT-ZnTAP and b) MWCNT-CuTAP

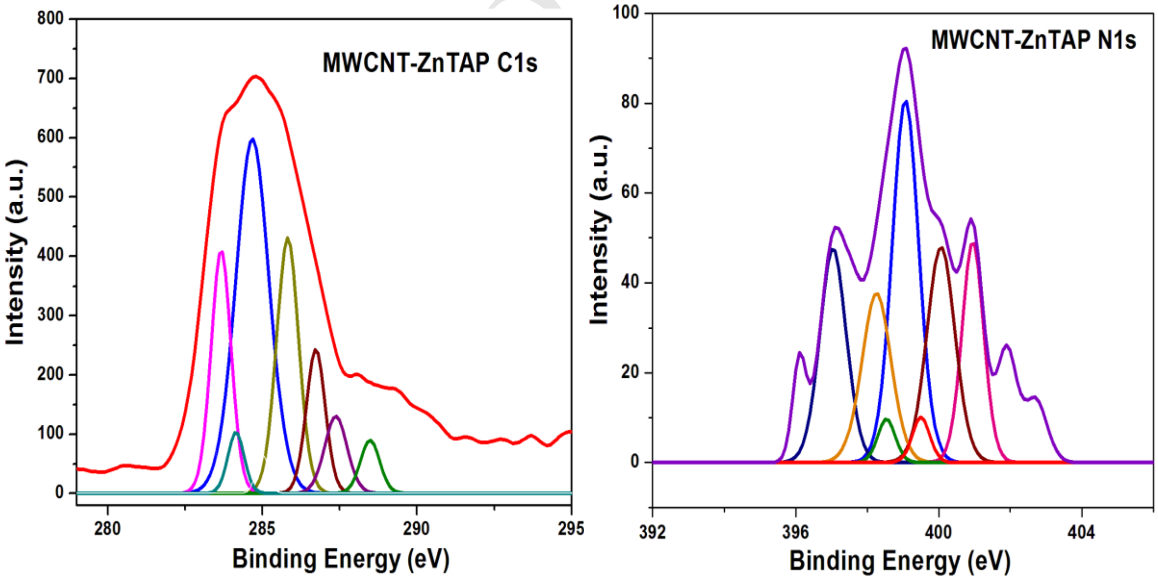

Figure.8. Deconvolutions of C 1s and N 1s for MWCNT-ZnTAP

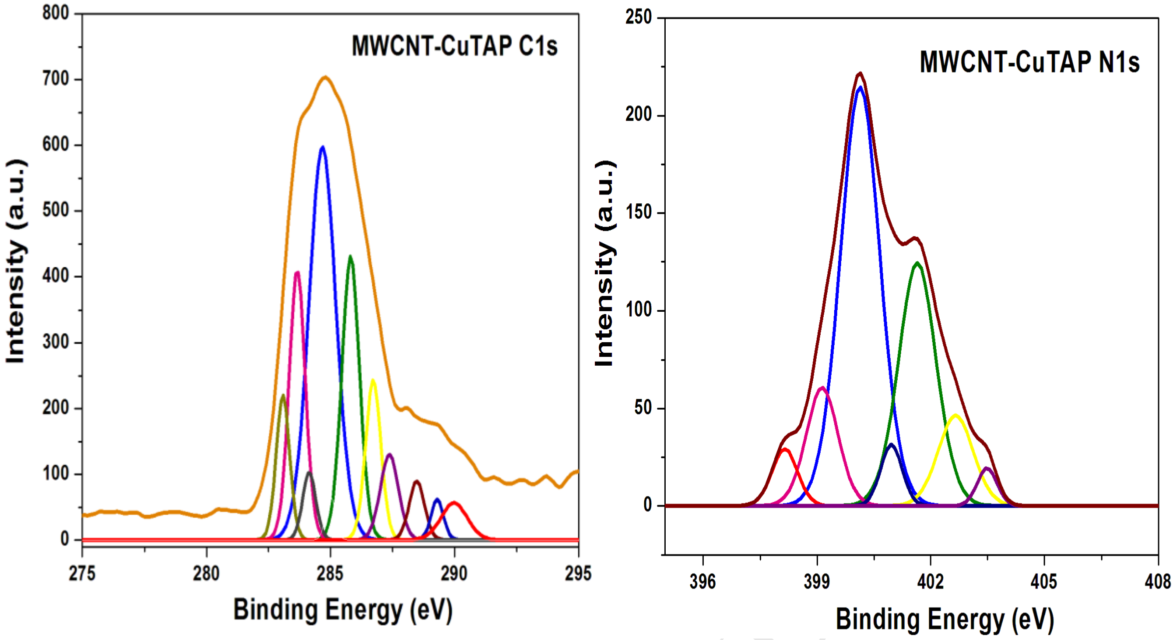

Figure.9. Deconvolutions of C 1s and N 1s for MWCNT-CuTAP

XPS has become an essential tool for the confirmation of elemental composition and further establish the electronic information of carbon nanomaterials. Figures 6 & 7 reveal the XP spectra of MWCNTs, MWCNT-COOH, MWCNT-ZnTAP and MWCNT-CuTAP. All samples demonstrate C 1s and O 1s peak. The presence of N 1s band and higher intensity O 1s band in the spectra of nano hybrids I and II denote the functionalization of organic molecules on the surface of MWCNTs. MWCNTs mainly contain carbon (94.51 %) and with low content of 5.49 % of oxygen (Figure 6a, Table 1). The presence of oxygen in MWCNTs is attributed to the atmospheric moisture that bound to the MWCNTs [19]. The C 1s spectrum of MWCNTs (see supporting information Figure S6a) exhibited four distinct peaks at 284.7, 284.9, 285.6 and 291.3 eV and these four peaks corresponds to sp^2 carbon atoms, defects on the nanotube structure, carbonyl (-C=O) groups and π–π* transition loss, respectively [20]. XP spectrum of MWCNT-COOH shows higher intensity O 1s band due to the oxidation of MWCNTs (Figure 6b, Table 1). We have find out the % of oxidization in MWCNTs using the peak position of oxygen containing functional groups from the literature [(C-OH (285.8 eV), O=C-O (288.9 eV), C=O (286.8 eV)] [27]. The % of oxidation (C-OH = 12.61 %, O=C-OH = 5.19 %, C=O = 4.31 %) was obtained by analyzing the C 1s region of MWCNT-COOH (see supporting information Figure

S6b). Some more new peaks were appeared in the C 1s XPS spectra of MWCNT-ZnTAP and MWCNT-CuTAP, after linking porphyrin to MWCNTs, indicating the covalent functionalization of MWCNTs with metallo porphyrins as shown in the Figures. 8 and 9. Furthermore covalent linking of metallo porphyrin with MWCNTs results in a considerable decrease in the intensity of C 1s peak of nano hybrids I and II relative to that of MWCNTs. The elemental composition obtained from XPS analysis were tabulated in the Table 1. Deconvolution of the N 1s spectrum of nano hybrids I and II exhibited the following contributions with the binding energies of 398.5, 400 and 398.1, 399.1 eV (sp^2 and sp^3 N atom bonded to Zn and Cu respectively) [28], and other peaks which corresponds to the C-N, N-H, C=N and N-C=O bonds as shown in the Figures.8 and 9. We estimated the % of metallo porphyrins linked with MWCNTs using the peak position of C-N (285.7 eV) and pyrolidinic nitrogen (400.2 eV)] [29]. The amount of Zn-TAP or Cu-TAP functionalized with MWCNTs are found to be 5.18 and 5.00 % using the C-N binding energy of nano hybrid I and II, respectively. Similarly, 2.14 and 3.26 % from the pyrolidinic nitrogen present in the nano hybrid I and II, respectively. Further XP spectra of nano hybrid I show new peaks related to Zn $2p_{1/2}$ and Zn $2p_{3/2}$ with the binding energies of 1044 and 1019 eV as shown in the inlet of Figure 7a. Whereas inlet of Figure 7b shows 4 peaks with binding energies of 935, 943, 954 and 962 eV for nano hybrid II which correspond to Cu $2p_{3/2}$, $2p_{3/2}$ satellite line, $2p_{1/2}$ and $2p_{1/2}$ satellite line, respectively [30]. Moreover these four peaks are slightly broad as compared to that of nano hybrid I which may be due to the paramagnetic nature of Cu. Thus XP spectra clearly indicates the covalent functionalization of Zn-TAP and Cu-TAP with MWCNTs.

Table. 1. Elemental composition [wt %] of pure MWCNTs, nano hybrid I and II obtained from XPS analysis (using areas of the respective peaks)

Sample	At wt %		
	C1s	O1s	N1s
MWCNT	94.51	5.49	-
MWCNT-COOH	79.14	20.86	-
MWCNT-ZnTAP	75.68	17.78	6.54
MWCNT-CuTAP	64.75	27.3	7.94

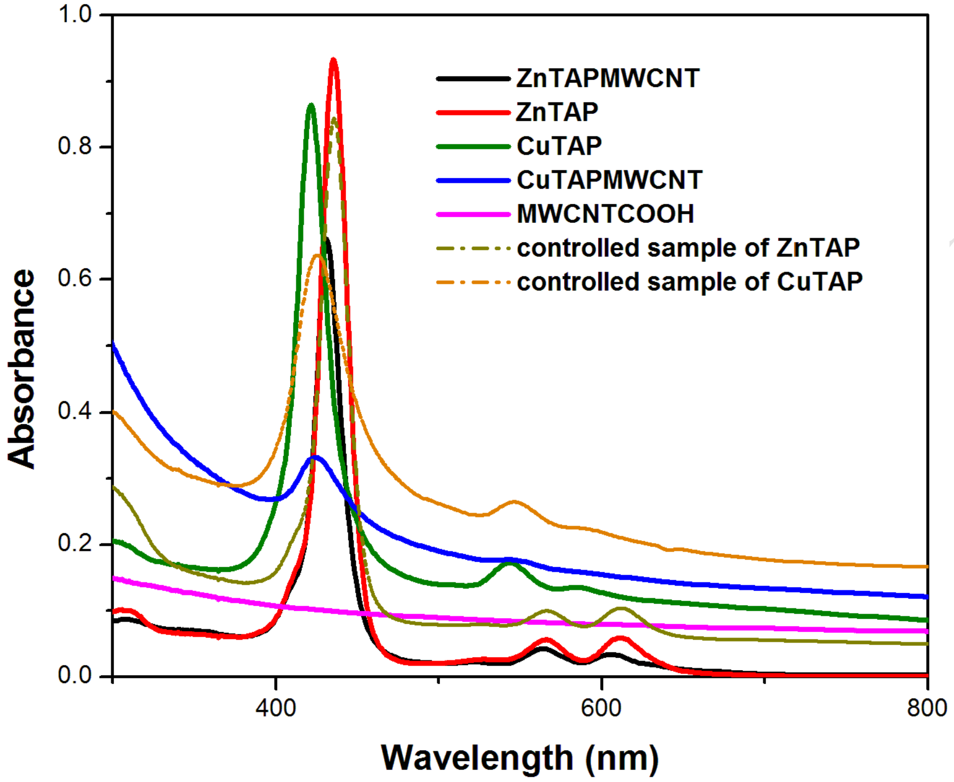

Figure.10. UV-vis absorption spectra with the 1cm path length for MWCNT-COOH (1 mg/100 mL), Zn-TAP (7.1 x 10^{-6} M), MWCNT-ZnTAP (0.7 mg/100mL), Cu-TAP (3.39 x 10^{-5} M), MWCNT-CuTAP (3.5 mg/100 mL) and controlled samples in DMF solvent

Figure 10 depicts UV-vis absorption spectra of MWCNT-COOH, Zn-TAP, Cu-TAP, physically blended sample of MWCNT-COOH with Zn-TAP or Cu-TAP (as a controlled sample, after sonicating the mixture for several hours), nano hybrids I and II in DMF solvent. Zn-TAP and Cu-TAP reveal a strong Soret band at 437 nm and 425 nm, respectively. Both the metal complexes show fewer Q peaks (two peaks) in the range 500 – 700 nm compared to porphyrin free base (TAP, 4 peaks). This is due to improved symmetry on metalation relative to the free base porphyrin from D_2h (rectangular) to D_4h (square) symmetry [24]. Generally, simpler spectrum results from more symmetrical molecule. Soret band of Cu-TAP and nano hybrid II show hypsochromic shift (blue shift) and also intensity of the peak is reduced (hypochromic shift) as compared to TAP, Zn-TAP and their nano hybrids. This is owing to the pronounced back bonding of paramagnetic Cu metal orbitals dπ (dxz and dyz) to porphyrin π* orbital [24]. However, zinc metal coordination to TAP affect the π-π* energy gap (slightly reduced) causing a slight red shift in both Zn-TAP and nano hybrid I (see table 2) compared to that of TAP and MWCNT-TAP. These findings clearly indicate that varying electronic energy level due to different metal ion substitution. Soret band of nano hybrids I and II reveal a blue shift as compared to pure Zn-TAP and Cu-TAP, respectively. This is evidence for the covalent linking of Zn-TAP or Cu-TAP with MWCNT [26]. Whereas there is no shift in the Soret band of physically blended samples as compared to metalloporphyrins. These nano hybrids also show improved solubility similar to MWCNT-TAP [22]. Detailed absorption studies in different solvents for example acetone, methanol, DMF, DMSO and THF have been carried out to indicate the charge transfer between Zn-TAP or Cu-TAP with MWCNTs. Nano hybrid I exhibits good solubility in all these solvents except THF (disperse after sonication). In order to determine the solubility, we plotted Soret band absorption value of nano-hybrid I in these solvents against concentrations to get a standard curve as given in the supporting information Figures S7 and S8. However, nano hybrid II is disperse well after sonication. Nano hybrids I and II, Zn-TAP and Cu-TAP reveal a red shift in the absorption spectra with increasing solvent polarity as shown in Table 2. However, the red shift is more pronounced in the case of nano hybrid I and Zn-TAP as compared to nano hybrid II and Cu-TAP. Consequently these nano hybrids also exhibit positive solvatochromism similar to the reported MWCNT-TAP [22]. Due to the formation hydrogen bond with the methanol, all these compounds exhibit blue shift in methanol.

Photoluminescence (PL) spectra of Zn-TAP, and nano hybrid I in DMF solvent are presented in the Figure 11. Upon excitation of Zn-TAP and nano hybrid I at 430 nm, the solution of MWCNT-ZnTAP exhibits ~62 % fluorescent quenching of emission peak at 622 nm as compared to that of pure Zn-TAP. This significant quenching is attributed to photo induced electron/energy transfer between Zn-TAP and MWCNTs of nano hybrid I [22]. Nano hybrid I displays two well resolved peaks at 622 nm and another at 676 nm with almost same intensity, whereas Zn-TAP shows broad peak at 633 nm with slight hump ~675 nm. Moreover, the peak of MWCNT-ZnTAP (622 nm) is blue shifted as compared to Zn-TAP (633 nm). These finding substantiates the covalent linking of Zn-TAP to MWCNT. The peaks of MWCNT-ZnTAP exhibit red shift as compared to the reported nano hybrid MWCNT-SnTPP [18]. This is due to the presence of electron donating amino group in the TAP moiety of nano hybrid I. Upon excitation at different wavelength the nano hybrid I exhibits similar quenching (82 %) for the peak at 633 nm as shown in Figure S9 (see supporting information λex = 450 nm). Nevertheless, the intensity of peak at 675 nm is increased by increasing the excitation wavelength. Fluorescence emission studies were performed in different solvents such as DMSO, DMF, methanol and THF at excitation wavelengths of 430 nm as shown in the Figure 12. Similar quenching was observed for MWCNT-ZnTAP in all these solvents. However, the intensity of the peak at 675 nm is varies with the polarity of solvent. This clearly indicates the effect of metal substitution which alter the electronic energy level of nano hybrid. We observed bathochromic shift (positive solvatochromism) by increasing the solvent polarity except in methanol which shows a blue shift due to hydrogen bonding [22]. Quantum yield (ϕ_F) for the Zn-TAP and MWCNT-ZnTAP were determined using TPP as reference at 20 ^oC (the measurement details are given in the supporting information). We found that the ϕ_F of Zn-TAP is 0.12 whereas the ϕ_F of MWCNT-ZnTAP is 0.08. The decrease in the ϕ_F is due to the charge transfer between Zn-TAP and MWCNT in the hybrid. However, no peaks were observed in the fluorescent spectra of Cu-TAP and MWCNT-CuTAP, due to paramagnetic effect of copper.

Table 2. Soret band peak position of Cu-TAP, MWCNT-CuTAP, Zn-TAP, and MWCNT-ZnTAP in different solvents

Solvent with decreasing polarity	Zn-TAP (in nm)	MWCNT-ZnTAP (in nm)	Cu-TAP (in nm)	MWCNT-CuTAP (in nm)
DMSO	440	434	425	425
DMF	437	432	425	423
Methanol	428	425	415	413
THF	433	429	420	416

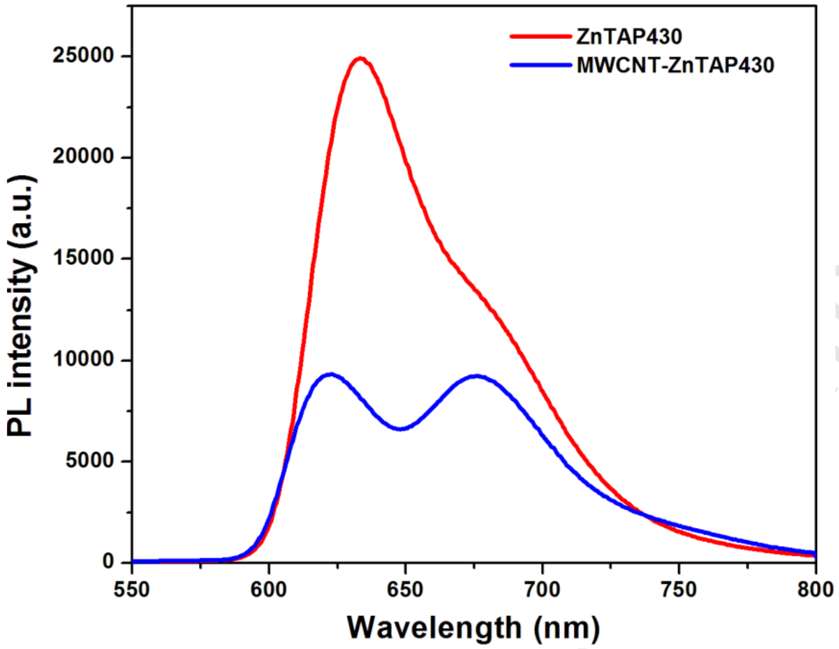

Figure.11. PL spectra of Zn-TAP and MWCNT-ZnTAP in DMF solvent (λex = 430 nm) with the same absorbance value at the Soret band (Abs = 0.24)

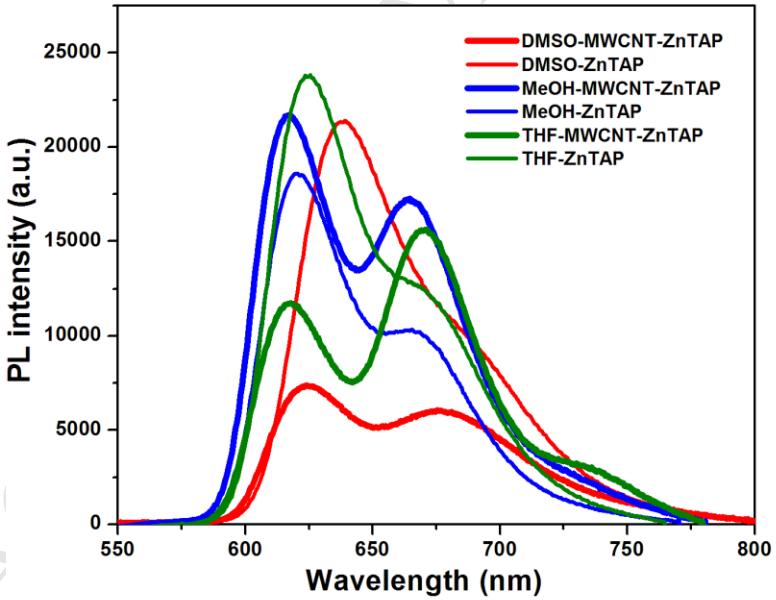

Figure.12. PL spectra of MWCNT-ZnTAP and Zn-TAP in different solvents (λex = 430 nm) with the same absorbance value at the Soret band (Abs = 0.24)

4. Conclusion

Zn and Cu tetraaminophenylporphyrin complexes were covalently connected with MWCNTs through an amide linkage. Significant modification in the FT-IR and XP spectra confirms the covalent functionalization of Zn-TAP and Cu-TAP with MWCNT. Raman spectra of MWCNT-ZnTAP and MWCNT-CuTAP exhibited higher frequency shift compared with MWCNT. This is possibly due to the metal co-ordination with TAP molecule. However, these nano hybrids exhibited slightly lower frequency shift compared with MWCNT-COOH. MWCNT-CuTAP shows more thermal stability compared to MWCNT-ZnTAP and also compared to the reported similar nano hybrids. Absorption spectra of Cu-TAP and its nano hybrid show blue shift due to the paramagnetic nature of Cu metal ion. Moreover, PL spectra of MWCNT-ZnTAP show, there is a fluorescence quenching of Zn-TAP Soret band by MWCNTs in various solvents. This quenching is owing to the covalent functionalization of Zn-TAP with MWCNT molecules in the nano hybrid. This further substantiates the energy or electron transfer between Zn-TAP and the MWCNTs.

Acknowledgements

We Thank COE-AMGT (MHRD, New Delhi) for their funding. We also thank Mr. S. Sarath, ACNSMM, AIMS Kochi for recoding XPS and Mr. Shibu, DST-SAIF, Kochi for recording TEM images.

Supporting Information available

NMR spectrum of Zn-TAP, EPR spectrum of Cu-TAP, IR spectra of nano hybrids I and II, Tem images, deconvolution peak of MWCNT & MWCNT-COOH C 1s, solubility studies, PL spectra of Zn-TAP and nano hybrid I in λex = 450 nm, ϕ_F measurement details.

References

[1] A. Schaetz, M. Zeltner, W. J. Stark, Carbon modifications and surfaces for catalytic organic transformation, (2012) ACS Catal 2:1267–1284.

[2] A. Muller, The chemistry of nanomaterials: synthesis, properties and application, (2004) Wiley-VCH, Weinheim

[3] M. Inagaki, K. Kaneko, T. Nishizawa, Nanocarbons-recent research in japan, (2004) Carbon, 42:1401-1417.

[4] Y. Yang, S. Chen, Q. Xue, A. Biris, W. Zhao, Electron transfer chemistry of octadecylamine-functionalized single-walled carbon nanotubes, (2005) Electrochim Acta 50:3061-3067.

[5] Y. Yin, Y. Lu, P. Wu and C. Cai, Direct electrochemistry of redox proteins and enzymes promoted by carbon nanotubes, (2005) Sensors 5: 220-234.

[6] Z. Wang, H. Lei, R. Cao, M. Zhang, Cobalt corrole on carbon nanotube as a synergistic catalyst for oxygen reduction reaction in acid media, (2015) Electrochim Acta 171:81–88.

[7] W. Zhang, A. U. Shaikh, E. Y. Tsui, and T. M. Swager, Cobalt porphyrin functionalized carbon nanotubes for oxygen reduction, (2009) Chemistry of Materials, 21(14), 3234–3241.

[8] M. E. Lipinska, S. L. H. Rebelo, and C. Freire, Iron (III) porphyrin anchored onto organosilylated multiwalled carbon nanotubes as an active catalyst for epoxidation reactions under mild conditions, (2014) Journal of Materials Science, 49(4), 1494–1505.

[9] W. Wei, H. H. Jin, G. C. Zhao, A reagentless nitrite biosensor based on direct electron transfer of hemoglobin on a room temperature ionic liquid/carbon nanotube-modified electrode, (2009) Microchim Acta, 164, 167-171.

[10] D. M. Guldi, G. M. A. Rahman, N. Jux, D. Balbinot, N. Tagmatarchis & M. Prato, Multiwalled carbon nanotubes in donor-acceptor nanohybrids - towards long-lived electron transfer products, (2005) Chem. Commun., 2038–2040.

[11] C. Ehli, D. M. Guldi, M. A. Herranz, N. Martín, S. Campidelli, & M. Prato, Pyrene-tetrathiafulvalene supramolecular assembly with different types of carbon nanotubes, (2008) Journal of Materials Chemistry 18(13), 1498.

[12] W. Lu, N. Li, W. Chen and Y. Yao, The role of multiwalled carbon nanotubes in enhancing the catalytic activity of cobalt tetraaminophthalocyanine for oxidation of conjugated dyes, (2009) Carbon 47, 3337

[13] X. Wang, B. Wang, J. Zhong, F. Zhao, N. Han, W. Huang, M. Zeng, J. Fan and Y. Li, Iron polyphthalocyanine sheathed multiwalled carbon nanotubes: A high-performance electrocatalyst for oxygen reduction reaction, (2016) Nano Research 9, 1497 .

[14] M. M. Stylianakis, D. Konios, G. Kakavelakis, G. Charalambidis, E. Stratakis, A. G. Coutsolelos, E. Kymakis and S. H. Anastasiadis, Efficient ternary organic photovoltaics incorporating grapheme -based porphyrin molecule as a universal electron cascade material, (2015) Nanoscale 7, 17827.

[15] L. Lu, T. Xu, W. Chen, E. S. Landry and L. Yu, Ternary blend polymer solar cells with enhanced power conversion efficiency, (2014) Nat. Photonics, 8, 716.

[16] J. Kesters, P. Verstappen, M. Kelchtermans, L. Lutsen, D. Vanderzande and W. Maes, Porphyrin-based bulk heterojunction organic photovoltaics: The rise of the colors of life, (2015) Adv. Energy Mater., 5, 1500218.

[17] D. M. Guldi and M. Prato, Excited-state properties of C60 fullerene derivatives, (2000) Acc. Chem. Res., 33, 695.

[18] A.Wang, J. Song, Z. Huang, Y. Song, W. Yu, H. Dong and J. Shao, Multi-walled carbon nanotubes covalently functionalized by axially coordinated metal-porphyrins: Facile syntheses and temporally dependent optical performance, (2016) Nano Research 9(2), 458-472.

[19] A. Wang, Y. Fang, W. Yu, L. Long, Y. Song, W. Zhao, C. Zhang, Allyloxyporphyrin-functionalized multiwalled carbon nanotubes: Synthesis by radical polymerization and enhanced optical-limiting properties, (2014) Chemistry - An Asian Journal 9(2), 639–648.

[20] A. Wang, Y. Fang, L. Long, Y. Song, W. Yu, W. Zhao, M. P. Cifuentes, M. G. Humphery and C. Zhang, Facile synthesis and enhanced nonlinear optical properties of porphyrin-functionalized multi-walled carbon nanotubes, (2013) Chem. Eur. J. 15 3882.

[21] M. B. M. Krishna, V. P. Kumar, N. Venkatramaiah, R. Venkatesan and D. N. Rao, Nonlinear optical properties of covalently linked graphene-metal porphyrin composite materials, (2011) Applied Physics Letters, 98(8).

[22] G. Prabhavathi, M. Arjun, R. Yamuna, Synthesis, characterization and photoluminescence properties of tetra (aminophenyl) porphyrin covalently linked to multi-walled carbon nanotubes, (2017) Journal of Chemical Sciences 129(6), 699-706.

[23] R. Boscencu, M. Ilie, R. Socoteanu, A. S. Oliveira, C. Constantin, M. Neagu, L. F. V. Ferreira, Microwave synthesis, basic spectral and biological evaluation of some copper (II) mesoporphyrinic complexes, (2010) Molecules, 15(5), 3731–3743.

[24] B. P. Bandgar, and, P. B. Gujarathi, Synthesis and Characterization of New Meso-Substituted and β-Substituted Unsymmetrical Metalloporphyrins, (2014) Chemical Science Transactions, 120(2), 259–266.

[25] K. Qu, H. Xu, C. Zhao, J. Ren and X. Qu, Amine-linker length dependent electron transfer between porphyrins and covalent amino-modified single-walled carbon nanotubes, (2011) RSC Adv. 1, 632.

[26] Z. Guo, F. Du, D. Ren, Y. Chen, J. Zheng, Z. Liu and J. Tian, Covalently porphyrin-functionalized single-walled carbon nanotubes: a novel photoactive and optical limiting donor-acceptor nanohybrid (2006) J. Mater. Chem. 16, 3021.

[27] K. A. Wepasnick, B .A. Smith, J. L. Bitter, D. H. Fairbrother, Chemical and structural characterization of carbon nanotube surfaces, (2009) Anal. Bioanal. Chem. 396(3), 1003-1014.

[28] D. K. Lavallee, J. Brace and N. Winograd, X-ray Photoelectron spectra of N-methyltetraphenyl porphyrins: evidence for a correlation of binding energies with metal-nitrogen bond distances, (1979) Inorganic chemistry, 18(7).

[29] T. Susi, T. Pichler, P. Ayala, X-ray photoelectron spectroscopy of graphitic carbon nanomaterials doped with heteroatoms, (2015) Beilstein. J. Nanotechnolgy 6, 177–192.

[30] M. Gopiraman, S. G. Babu, Z. Khatri, W.Kai, Y. A. Kim, M. Endo, R. Karvembu, I. S. Kim, An efficient, reusable copper-oxide/carbon-nanotube catalyst for N-arylation of imidazole, (2013) Carbon, 62, 135-148.

Highlights

- Zn and Cu tetraaminophenylporphyrin complexes were covalently connected with MWCNTs.
- Significant modification in the FT-IR and XP spectra confirms the covalent functionalization of Zn-TAP and Cu-TAP with MWCNT.
- These nano-hybrids exhibit positive solvatochromism
- PL spectra of MWCNT-ZnTAP exhibited fluorescence quenching of Zn-TAP Soret band by MWCNTs in various solvents.